ORIGINAL ARTICLE

Cancer Science WILEY

Tumor microenvironmental 15-PGDH depletion promotes fibrotic tumor formation and angiogenesis in pancreatic cancer

Luke Bu[1,2] | Atsuko Yonemura[1,2] | Noriko Yasuda-Yoshihara[1,2] | Tomoyuki Uchihara[1] |
Galym Ismagulov[3] | Sanae Takasugi[4] | Tadahito Yasuda[2] |
Yuya Okamoto[1] | Fumimasa Kitamura[1,2] | Takahiko Akiyama[1,2] | Kota Arima[1] |
Rumi Itoyama[1] | Jun Zhang[1,2] | Lingfeng Fu[1,2] | Xichen Hu[1,2] | Feng Wei[1,2] |
Yuichiro Arima[5] | Toshiro Moroishi[6,7] | Koichi Nishiyama[8] | Guojun Sheng[3] |
Toshifumi Mukunoki[9] | Jun Otani[9] | Hideo Baba[1,7] | Takatsugu Ishimoto[1,2]

[1]Department of Gastroenterological Surgery, Graduate School of Medical Sciences, Kumamoto University, Kumamoto, Japan

[2]Gastrointestinal Cancer Biology, International Research Center of Medical Sciences (IRCMS), Kumamoto University, Kumamoto, Japan

[3]Developmental Morphogenesis, IRCMS, Kumamoto University, Kumamoto, Japan

[4]Application Department, X-ray Division, Bruker Japan K.K., Kanagawa, Japan

[5]Developmental Cardiology, IRCMS, Kumamoto University, Kumamoto, Japan

[6]Department of Cell Signaling and Metabolic Medicine, Faculty of Life Sciences, Kumamoto University, Kumamoto, Japan

[7]Center for Metabolic Regulation of Healthy Aging, Faculty of Life Sciences, Kumamoto University, Kumamoto, Japan

[8]Laboratory of Vascular and Cellular Dynamics, Department of Medical Sciences, University of Miyazaki, Miyazaki City, Japan

[9]X-Earth Center, Faculty of Advanced Science and Technology Kumamoto University, Kumamoto, Japan

Correspondence
Takatsugu Ishimoto and Hideo Baba, Department of Gastroenterological Surgery, Graduate School of Medical Sciences, Kumamoto University, 1-1-1 Honjo, Chuo-ku, Kumamoto 860-8556, Japan.
Emails: taka1516@kumamoto-u.ac.jp (TI); hdobaba@kumamoto-u.ac.jp (HB)

Funding information
Japan Science and Technology Agency, Grant/Award Number: JPMJFR200H; Japan Society for the Promotion of Science, Grant/Award Number: 20H03531, 20K08985, 20K09038 and 21K19535; Naito Foundation; The Shinnihon Foundation of Advanced Medical Treatment Research

Abstract

The arachidonic acid cascade is a major inflammatory pathway that produces prostaglandin E_2 (PGE2). Although inhibition of 15-hydroxyprostaglandin dehydrogenase (15-PGDH) is reported to lead to PGE2 accumulation, the role of 15-PGDH expression in the tumor microenvironment remains unclear. We utilized Panc02 murine pancreatic cancer cells for orthotopic transplantation into wild-type and 15-pgdh$^{+/-}$ mice and found that 15-pgdh depletion in the tumor microenvironment leads to enhanced tumorigenesis accompanied by an increase in cancer-associated fibroblasts (CAFs) and the promotion of fibrosis. The fibrotic tumor microenvironment is widely considered to be hypovascular; however, we found that the angiogenesis level is maintained in 15-pgdh$^{+/-}$ mice, and these changes were also observed in a genetically engineered PDAC mouse model. Further confirmation revealed that fibroblast growth factor 1 (FGF1) is secreted by pancreatic cancer cells after PGE2 stimulation, consequently promoting CAF proliferation and vascular endothelial growth factor A (VEGFA)

Abbreviations: 15-PGDH, 15-hydroxyprostaglandin dehydrogenase; CAFs, cancer-associated fibroblasts; COX-2, cyclooxygenase 2; FGF1, fibroblast growth factor 1; NK cells, natural killer cells; PanIN, precancerous lesions; PDAC, pancreatic ductal adenocarcinoma; PGE2, prostaglandin E_2; Tregs, regulatory T cells; VEGFA, vascular endothelial growth factor A; αSMA, alpha-smooth muscle actin.

expression in the tumor microenvironment. Finally, in 15-pgdh$^{+/-}$Acta2-TK mice, depletion of fibroblasts inhibited angiogenesis and cancer cell viability in orthotopically transplanted tumors. These findings highlighted the role of 15-pgdh downregulation in enhancing PGE2 accumulation in the pancreatic tumor microenvironment and in subsequently maintaining the angiogenesis level in fibrotic tumors along with CAF expansion.

KEYWORDS
cancer-associated fibroblasts, prostaglandin E$_2$, tumor microenvironment

1 | INTRODUCTION

Pancreatic ductal adenocarcinoma (PDAC) is one of the most serious malignant diseases.[1] Despite the development of anticancer treatments in recent decades, PDAC remains the seventh leading cause of cancer death in individuals of all ages regardless of sex worldwide.[2] Pancreatic cancer often tends to be asymptomatic in the early stage and is diagnosed at an advanced stage; therefore, only 20% of patients are candidates for surgical resection.[3,4] Pancreatic cancer is also recognized to have a highly fibrotic tumor microenvironment with relatively few infiltrated immune cells; this major pathological feature causes an elevated interstitial pressure in PDAC tumors and inevitably compresses the blood vessels in the stroma, creating a hypovascular and hypoxic tumor microenvironment.[5,6]

Various factors, including alcohol, smoking, obesity, and so forth, contribute to pancreatic cancer initiation and progression.[7] Most of these risk factors can trigger an inflammatory response; for example, smoking can release carcinogens and accelerate the process of chronic pancreatitis,[8] and the obesity-induced central fat distribution has been associated with a systemic inflammatory response in patients with acute pancreatitis.[9]

During inflammation and cancer progression, the common pathological features of chronic inflammatory diseases and solid cancers include elevated levels of proinflammatory mediators such as cytokines, chemokines, and lipids, including increased expression of both prostaglandin E$_2$ (PGE2) in the arachidonic acid cascade and cyclooxygenase 2 (COX-2), a key enzyme in PGE2 synthesis.[10] PGE2 was previously reported to play a crucial role in regulating tissue regeneration and hematopoietic stem cell homeostasis.[11,12] In addition to being found in normal tissue, PGE2 and its related enzymes are routinely identified in a variety of tumor tissues in humans and animals, and

PGE2 contributes to tumor initiation, proliferation, and metastasis.[13] Depletion of 15-hydroxyprostaglandin dehydrogenase (15-PGDH), the enzyme catalyzing the degradation of PGE2, leads to PGE2 accumulation and expands the cancer stem cell population, subsequently promoting tumorigenesis.[14] Although several studies have shown the roles of 15-PGDH in various tissues, including cancer tissue,[15,16] its impact on the tumor microenvironment remains unknown. This study aims to elucidate the role of 15-PGDH as a PGE2-degrading enzyme in the tumor microenvironment, further revealing the link between PGE2 accumulation and pancreatic cancer stromal remodeling.
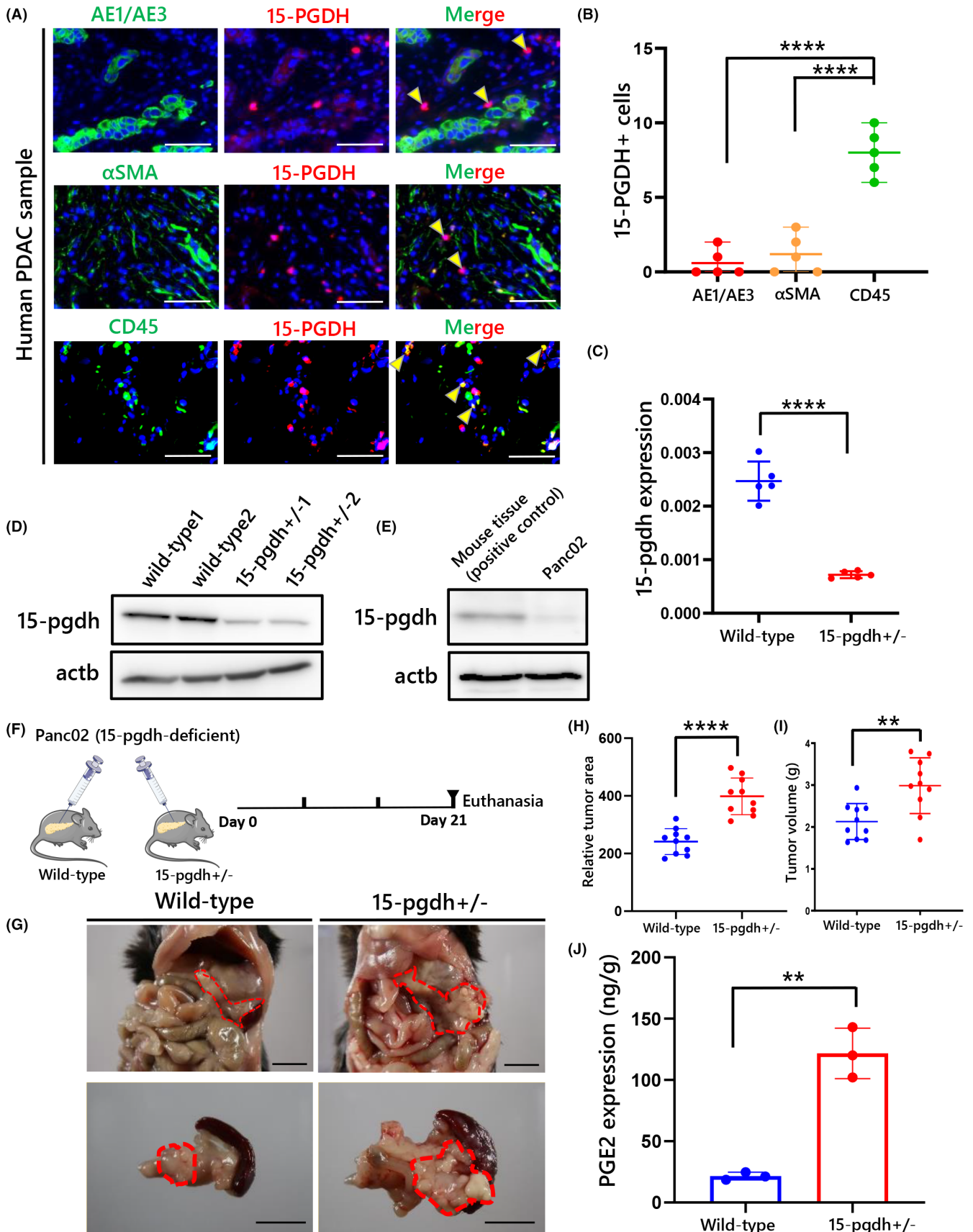
2 | MATERIALS AND METHODS

2.1 | Patients and tissue samples

Primary PDAC tissues were obtained from 121 consecutive PDAC patients who underwent radical pancreatic resection at Kumamoto University Hospital between April 2002 and June 2014. Written informed consent to participate was obtained from all patients. The study was approved by the Medical Ethics Committee of Kumamoto University (Approval Number: 1291).

2.2 | Cell lines and cell culture

The human PDAC cell lines PANC1, PK59, PK-8, AsPC1, and MIAPaCa2 were obtained from the Japanese Collection of Research Bioresources Cell Bank and RIKEN Bioresource Center Cell Bank. Panc02 cells were available from the ATCC. Cancer-associated fibroblasts (CAFs) were established from resected tissues collected from patients with

FIGURE 1 15-PGDH is expressed in the tumor microenvironment and promotes tumorigenesis of PDAC. (A) Representative immunofluorescence staining for 15-PGDH, AE1/AE3, αSMA and CD45. The arrowheads show strongly 15-PGDH-positive cells. Scale bars, 100 μm. (B) Quantification of AE1/AE3$^+$, αSMA$^+$ and CD45$^+$ cells. (C, D) 15-pgdh expression in 15-pgdh$^{+/-}$ mice and wild-type mice was evaluated by qRT-PCR (C) and western blotting (D). (E) Expression of 15-pgdh in Panc02 cell lines and normal spleen tissue was evaluated by western blotting. (F) Strategy used to establish the orthotopic transplantation model. Panc02 cells deficient in 15-pgdh were injected into the pancreas of wild-type and 15-pgdh$^{+/-}$ mice to generate orthotopic xenografts. After 21 days, the mice were euthanized, and the tumors were harvested and weighed. (G) Images showing pancreatic tumors and spleens. Scale bars, 1 cm. (H) Main tumor area of wild-type and 15-pgdh$^{+/-}$ mice measured by ImageJ software. (I) Volumes of tumors from wild-type and 15-pgdh$^{+/-}$ mice. (J) PGE2 expression was measured by LC/MS in wild-type mice and 15-pgdh$^{+/-}$ mice. NS, not significant; **$p < 0.01$; ***$p < 0.001$; ****$p < 0.0001$

(A) Human PDAC sample — AE1/AE3, 15-PGDH, Merge; αSMA, 15-PGDH, Merge; CD45, 15-PGDH, Merge

(B) 15-PGDH+ cells: AE1/AE3, αSMA, CD45; **** ****

(C) 15-pgdh expression: Wild-type vs 15-pgdh+/−; ****

(D) wild-type1, wild-type2, 15-pgdh+/−1, 15-pgdh+/−2; 15-pgdh; actb

(E) Mouse tissue (positive control), Panc02; 15-pgdh; actb

(F) Panc02 (15-pgdh-deficient); Wild-type, 15-pgdh+/−; Day 0 — Day 21 Euthanasia

(G) Wild-type, 15-pgdh+/−

(H) Relative tumor area: Wild-type vs 15-pgdh+/−; ****

(I) Tumor volume (g): Wild-type vs 15-pgdh+/−; **

(J) PGE2 expression (ng/g): Wild-type vs 15-pgdh+/−; **

pancreatic cancer at Kumamoto University. The detailed protocol used to establish these cell lines has been reported previously.[17,18] These cell lines were cultured in RPMI 1640 medium containing 10% FBS and maintained at 37°C in a humidified atmosphere containing 5% CO_2.

PBMCs were obtained from the whole blood of healthy volunteers by centrifugation. Magnetic-activated cell sorting (MACS) was used to acquire CD14+ monocytes from PBMCs, and these were induced to differentiate into immature macrophages by macrophage colony
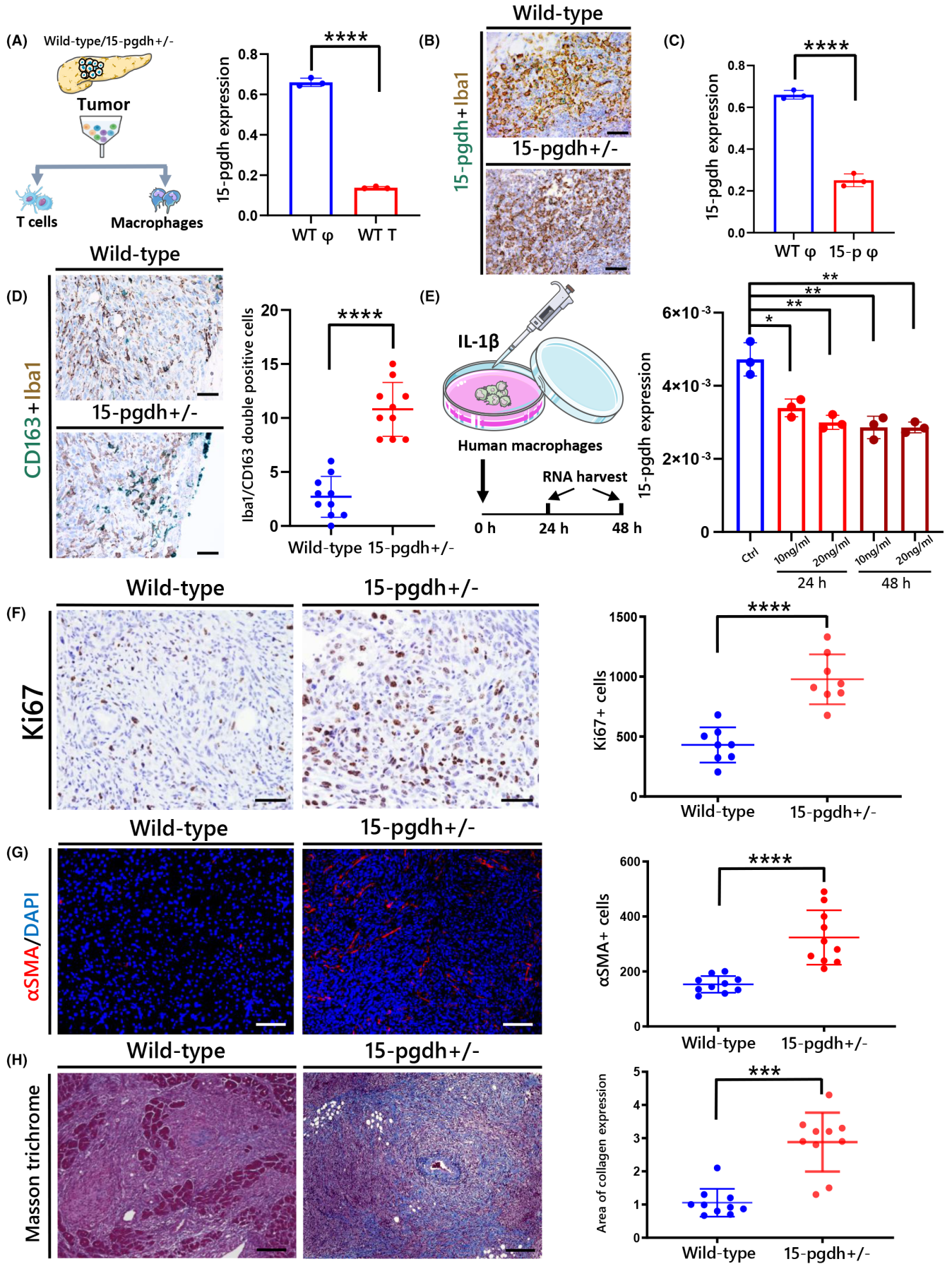
FIGURE 2 15-PGDH deficiency in macrophages causes tumor proliferation and fibrosis elevation. (A) Strategy used for cell sorting from tumors and 15-pgdh expression in sorted T cells and macrophages. WT, wild-type; φ, macrophages; T, T cells. (B) Double immunohistochemical staining of 15-pgdh and the mouse macrophage marker Iba1 in wild-type and 15pgdh$^{+/-}$ mice. Scale bars, 50 μm. (C) 15-pgdh expression in sorted T cells and macrophages. WT, wild-type; 15p, 15-pgdh$^{+/-}$; φ, macrophages. (D) Double immunohistochemical staining of Iba1 and CD163 in wild-type and 15pgdh$^{+/-}$ mice. Scale bars, 50 μm. (E) Sketch map of the IL-1β treatment of macrophages and 15-PGDH expression in human macrophages. (F) Representative immunohistochemical staining for Ki67 in wild-type and 15-pgdh$^{+/-}$ mouse tumors. The graph on the right shows the quantification of Ki67$^+$ cells. Scale bars, 200 μm. (G) Representative immunofluorescence staining for αSMA in wild-type and 15-pgdh$^{+/-}$ mouse tumors. The graph on the right shows the quantification of αSMA$^+$ cells. Scale bars, 50 μm. (H) Representative Masson's trichrome staining of wild-type and 15-pgdh$^{+/-}$ mouse tumors. The graph on the right shows the area of collagen expression. Scale bars, 200 μm. **$p < 0.01$; ***$p < 0.001$; ****$p < 0.0001$

stimulating factor 1 (M-CSF) (50 ng/ml). Macrophages were treated with distilled water (DW) or recombinant IL-1β (10 ng/ml or 20 ng/ml), and total RNA was harvested after 24 and 48 h of treatment.

2.3 | Animal statement

All experimental protocols were approved by the Ethical Review Board of the Graduate School of Medicine, Kumamoto University (Approval no. 2020-018R1) and were performed in accordance with the committee guidelines and regulations. Efforts were made to meet the scientific goals of this study with the minimum number of animals. Here, 6- to 8-week-old male or female C57BL/6N mice (Clea Japan) were housed in a room maintained at a stable temperature and humidity on a 12-h light/dark cycle. Mice were randomly assigned to the control and experimental groups for subsequent drug treatment. All experimental groups were assigned based on the genotype. 15-pgdh-deficient mice (15pgdh$^{+/-}$, 15pgdh$^{-/-}$) and 15-pgdh$^{-/-}$; Kras$^{LSL-G12D/+}$; Ptf1a$^{Cre/+}$ (referred to as PgKC) mice on a C57BL/6N background were generated as described previously.[14] Acta2-TK mice were purchased from ©The Jackson Laboratory (stock no. 029921). Ganciclovir (InvivoGen, 82410–32-0) was administrated to wild-type Acta2-TK mice and 15pgdh$^{+/-}$ Acta2-TK mice (50 mg/kg/day) at 7 weeks of age, 7 days later transplantation was performed, and the administration of Ganciclovir (GCV) was retained until the harvest of tumors (additional 3 weeks).

2.4 | Syngeneic transplantation of Panc02 cells and depletion of CAFs

Panc02 cells were suspended in cold RPMI 1640 medium. Wild-type and 15pgdh$^{+/-}$ mice were anesthetized by i.p. injection with triple anesthesia (0.75 mg/kg Domitor, 4 mg/kg Dormicum, and 5 mg/kg butorphanol). After local shaving and disinfection, the abdominal cavity was opened by a longitudinal incision ~1.5 cm below the right thoracic rib, the tail of the pancreas was confirmed by lifting the spleen, and 1×10^6 Panc02 cells in 60 μl of RPMI 1640 medium were injected using a 31-G needle. To further prevent leakage, the needle was held at the injection site for 30 s before removal. Postoperatively, the peritoneum and skin were sutured, and an analgesic (1–2 mg/kg Betorfar, subcutaneous administration once every 4 h×3 doses) was administered. For Acta2-TK mice, 50 mg/kg/day ganciclovir was administered i.p. for 3 weeks. All

mice were sacrificed 21 days after transplantation, and pancreas and spleen samples were harvested for further examination.

2.5 | Study approval

This research was approved by the Medical Ethics Committee of Kumamoto University. Written informed consent to participate in this study was obtained from all patients.

2.6 | Supplumentary Material and Methods

Details of other material and methods are clarified in Appendix S1.

3 | RESULTS

3.1 | 15-PGDH is found in the tumor microenvironment, and depletion of 15-PGDH promotes tumorigenesis

To investigate the source of 15-PGDH, we first performed immunofluorescence staining for 15-PGDH, AE1/AE3, αSMA and CD45 (Figure 1A). Despite its weak expression in AE1/AE3$^+$ tumor cells, 15-PGDH was expressed mainly in the tumor microenvironment, specifically in CD45$^+$ cells (Figure 1B). Consistent with the above results, we demonstrated that 15-PGDH was found predominantly in the tumor microenvironment rather than in tumor cells. Therefore, to further examine the effect of 15-pgdh depletion in the tumor microenvironment, we developed 15pgdh knockout mice (15-pgdh$^{-/-}$ mice).[14] Notably, 15-pgdh knockout in mice has been shown to lead to postnatal lethality via the ductus arteriosus, and indomethacin treatment can rescue these mice after birth.[19] However, as the successful rescuing rate is extremely inadequate for 15-pgdh$^{-/-}$ mice, we utilized 15-pgdh$^{+/-}$ mice and established a syngeneic transplantation mouse model using the murine pancreatic cancer cell line Panc02. First, we confirmed the drastic downregulation of 15-pgdh expression in 15-pgdh$^{+/-}$ mice compared with wild-type mice at both the mRNA (Figure 1C) and protein (Figure 1D) levels. As we want to avoid the influence of 15-pgdh from cancer cells in our transplantation model, so that we can focus more on the tumor microenvironment, we also confirmed 15-pgdh expression levels in
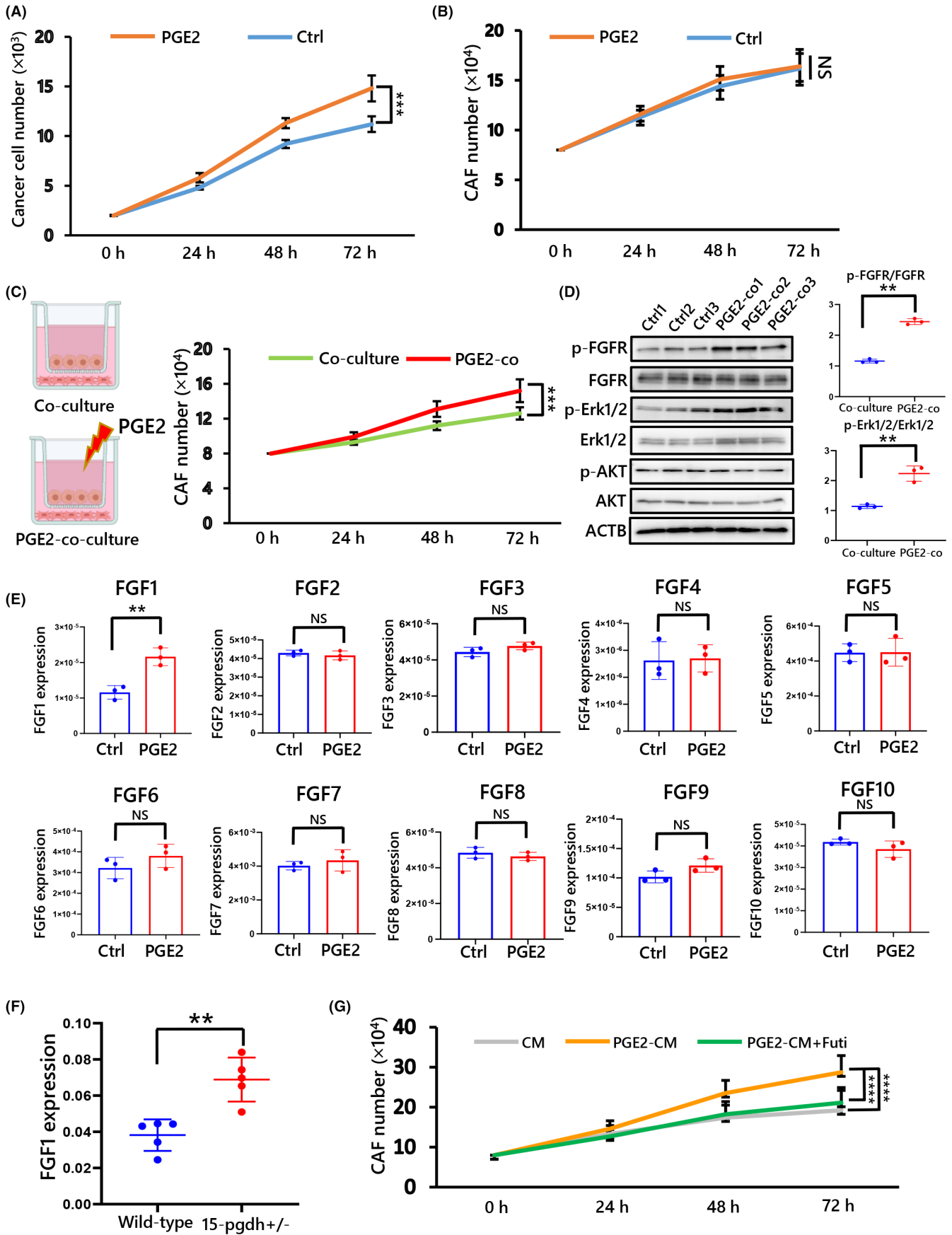
FIGURE 3 CAF proliferation and fibrosis are enhanced after 15-pgdh ablation. (A, B) The number of PK8 cells (A) or CAFs (B) after DMSO (Ctrl) or PGE2 treatment. (C) Image of the Transwell system used to coculture PK8 cells with CAFs and the number of CAFs after DMSO (Ctrl) or PGE2 treatment. (D) FGF, FGFR, AKT, phosphorylated AKT, Erk1/2, and phosphorylated Erk1/2 were examined by Western blotting. (E) Expression of each FGF in PK8 cells after DMSO (Ctrl) or PGE2 treatment. (F) FGF1 expression in tumors derived from Panc02 cells transplanted into wild-type and 15-pgdh$^{+/-}$ mice. (G) Number of CAFs after culture with PK8 cell CM supplemented with DMSO (Ctrl), PGE2 or PGE2$^+$ futibatinib (Futi). NS, not significant; **$p < 0.01$; ***$p < 0.001$; ****$p < 0.0001$

Panc02 cells using normal spleen tissue from wild-type mice as a positive control (Figure 1E). Panc02 cells do not express 15-pgdh and therefore can be used as a 15-pgdh-depleted cell line. The strategy used to establish the orthotopic transplantation model is shown in Figure 1F. By transplanting the same 15-pgdh-deficient Panc02 cells into wild-type and 15-pgdh$^{+/-}$ mice, we created two types of tumor microenvironments with different levels of 15-pgdh expression. Notably, after wild-type and 15-pgdh$^{+/-}$ mice were sacrificed 3 weeks after Panc02 cell transplantation, we found that the pancreases and spleens were significantly larger in 15-pgdh$^{+/-}$ mice than in wild-type mice and that these increases in organ size were accompanied by large increases in tumor size (Figure 1G,H) and tumor weight (Figure 1I). Then, we examined the accumulation of PGE2 in both genotypes of mice by LC/MS. As expected, PGE2 dramatically accumulated in 15-pgdh$^{+/-}$ mice (Figure 1J). The above results suggested that 15-PGDH is expressed mainly in the tumor microenvironment rather than in cancer cells and that depletion of 15-PGDH can lead to PGE2 accumulation, consequently promoting tumor enlargement.

3.2 | 15-PGDH deficiency in macrophages causes tumor proliferation and enhances fibrosis

We assumed that the phenomenon above was caused by 15-pgdh ablation in the tumor microenvironment, and we next conducted FACS to further identify the source of 15-pgdh. Recent studies have reported that 15-pgdh is mainly expressed by macrophages and regulatory T (Treg) cells in muscle microenvironments and visceral adipose tissue,[20,21] and based on this information and our former immunofluorescence staining data, we sorted T cells (CD3$^+$) and macrophages (F4/80$^+$) from tumors from both genotypes of mice and analyzed them by real-time PCR. Here, 15pgdh was expressed predominantly by macrophages rather than T cells in transplanted tumors in wild-type mice (Figure 2A and Figure S1), providing evidence that macrophages are the main source of 15pgdh. In addition, double immunohistochemical staining for 15-pgdh and the mouse macrophage marker Iba1 showed the same phenomenon; most Iba1$^+$ cells in wild-type mice expressed 15-pgdh, whereas in 15pgdh$^{+/-}$ mice, among the Iba1-positive cells, very few 15pgdh-positive cells were detected (Figure 2B). We also confirmed the markedly decreased expression of 15-pgdh in macrophages in 15-pgdh$^{+/-}$ mice at the mRNA level (Figure 2C). To examine the features of those macrophages, we performed double staining of Iba1 and CD163 and consequently found that CD163-positive macrophages were significantly increased in 15pgdh$^{+/-}$ tumor tissues compared with those in wild-type, suggesting that

M2-like macrophages are increased in 15-pgdh$^{+/-}$ mice (Figure 2D). Moreover, our previous study has shown that 15-PGDH can be downregulated by IL-1β in pancreatic cancer cells.[22] In addition, given that the data above suggested that tumor-infiltrating macrophages are the dominant source of 15-PGDH in the tumor microenvironment, we isolated monocytes, differentiated them into macrophages, and examined whether the expression of 15-PGDH in macrophages is also downregulated. Consequently, we found that 15-PGDH expression in macrophages was downregulated by IL-1β treatment, indicating that 15-PGDH from macrophages is downregulated by IL-1β in the tumor microenvironment the same as in pancreatic cancer cells (Figure 2E). To further examine the influence of 15-pgdh depletion, we conducted multiple evaluations using tissue from transplanted tumors in mice. Pathological examination of the solid tumors revealed that Ki67 expression was highly upregulated in multiple areas in 15-pgdh$^{+/-}$ mice (Figure 2F), indicating the presence of excessively proliferating tumor cells. Since the tumors that formed in our transplantation model were solid and stiff, we next examined the fibrosis level in the tumors. Immunofluorescence staining for αSMA revealed that the number of CAFs was significantly elevated in 15-pgdh$^{+/-}$ mice compared with wild-type mice (Figure 2G). Moreover, via Masson's trichrome staining, we found that collagen expression was drastically enhanced in 15-pgdh$^{+/-}$ mouse tumors (Figure 2H). These findings indicated that 15-pgdh is produced mainly by macrophages in the tumor microenvironment and that ablation of 15-pgdh induces tumor proliferation accompanied by enhanced fibrosis.

3.3 | The proliferation of CAFs is enhanced through fibroblast growth factor 1 (FGF1)-fibroblast growth factor receptor (FGFR) signaling

Because αSMA$^+$ and Ki67$^+$ cells were clearly increased in 15-pgdh$^{+/-}$ mice, we first hypothesized that the proliferation of CAFs or cancer cells is promoted by PGE2 accumulation due to 15-pgdh deficiency. Therefore, we treated CAFs and the pancreatic cancer cell line PK8, established from PDAC patients, with PGE2. The growth of PK8 cells was boosted by PGE2 treatment after 72 h of *in vitro* culture (Figure 3A); however, no significant change in the proliferation of CAFs was observed after 72 h of direct PGE2 treatment (Figure 3B). As the Prostaglandin E2 receptor (EP) family, the receptors for PGE2, can also be found in cancer cells, we next hypothesized that in the context of cancer, PGE2 stimulates cancer cells rather than directly impacting CAFs. To test this hypothesis, we used a Transwell system to coculture PK8 cells with

CAFs. Notably, CAF proliferation was considerably increased after coculture with PGE2-treated PK8 cells (Figure 3C). To investigate the reason for the enhanced CAF proliferation, we examined the intracellular signaling involved in CAF growth using lysates from cocultured CAFs. Western blot analysis showed increases in the levels of phosphorylated FGFR and phosphorylated Erk1/2, indicating that FGFR is potentially essential in promoting CAF proliferation (Figure 3D). To further verify the ligand that binds to FGFR,
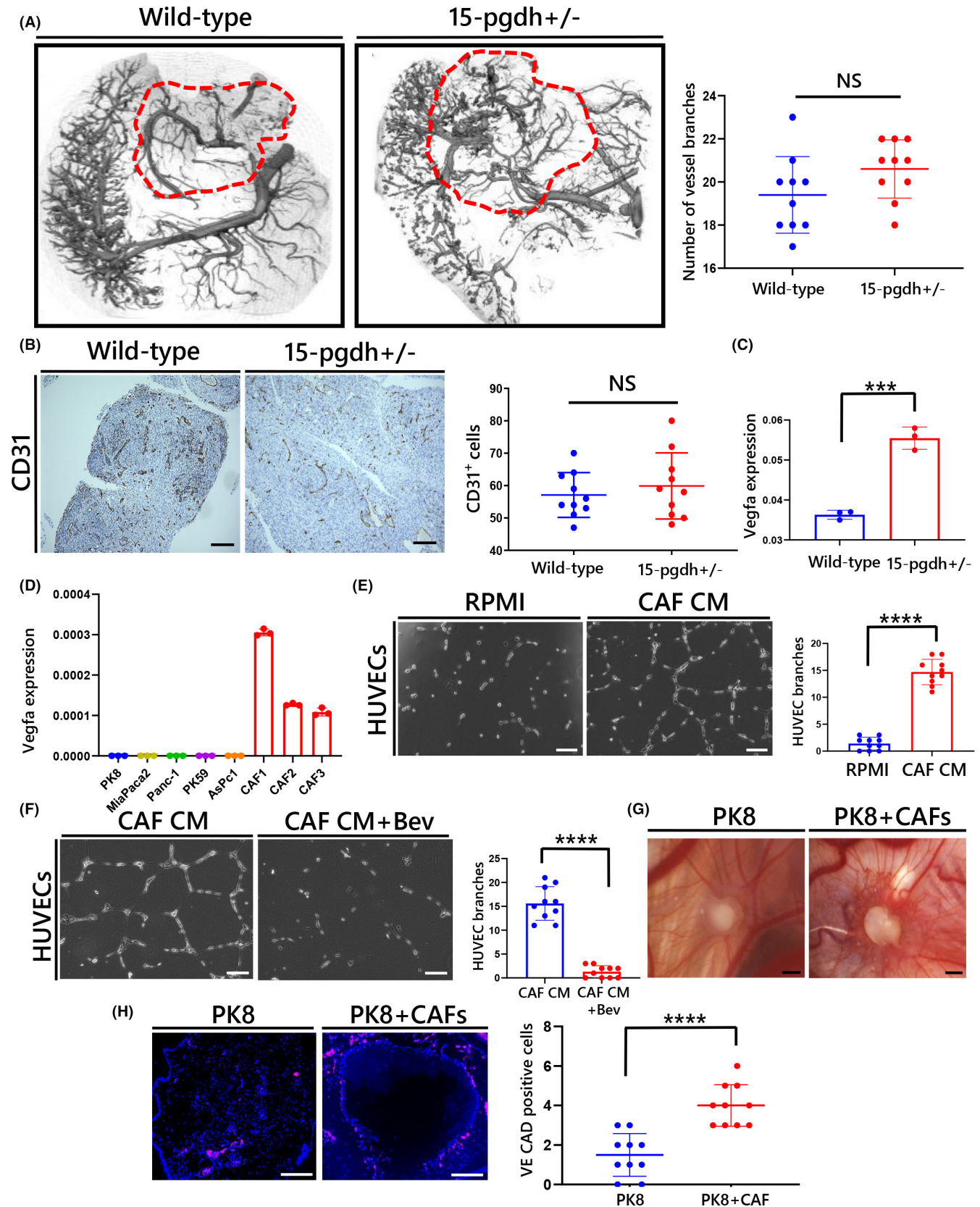
FIGURE 5 Genetic deletion of 15-pgdh favors fibrosis and angiogenesis in a PDAC mouse model. (A) Images showing pancreatic tumors and spleens of KC and PgKC mice. Main pancreas area of KC and PgKC mice measured by ImageJ. Scale bars, 1 cm. (B) H&E staining of KC and PgKC mice, Scale bars, 200 μm. (C) Representative Masson's trichrome staining of KC and PgKC mouse tumors. The graph on the right shows the area of collagen expression. KC: Kras$^{LSL-G12D/+}$; PgKC, Ptf1aCre$^{/+}$mice: 15pgdh$^{-/-}$; Kras$^{LSL-G12D/+}$; Ptf1aCre$^{/+}$mice. Scale bars, 500 μm. (D) Representative immunofluorescence staining for αSMA in KC and PgKC mice. The graph on the right shows the quantification of αSMA$^+$ cells. Scale bars, 50 μm. (E) Representative immunohistochemical staining for CD31 and quantification of CD31$^+$ cells in KC and PgKC mice, Scale bars, 50 μm. NS, not significant; **$p < 0.01$; ***$p < 0.001$; ****$p < 0.0001$
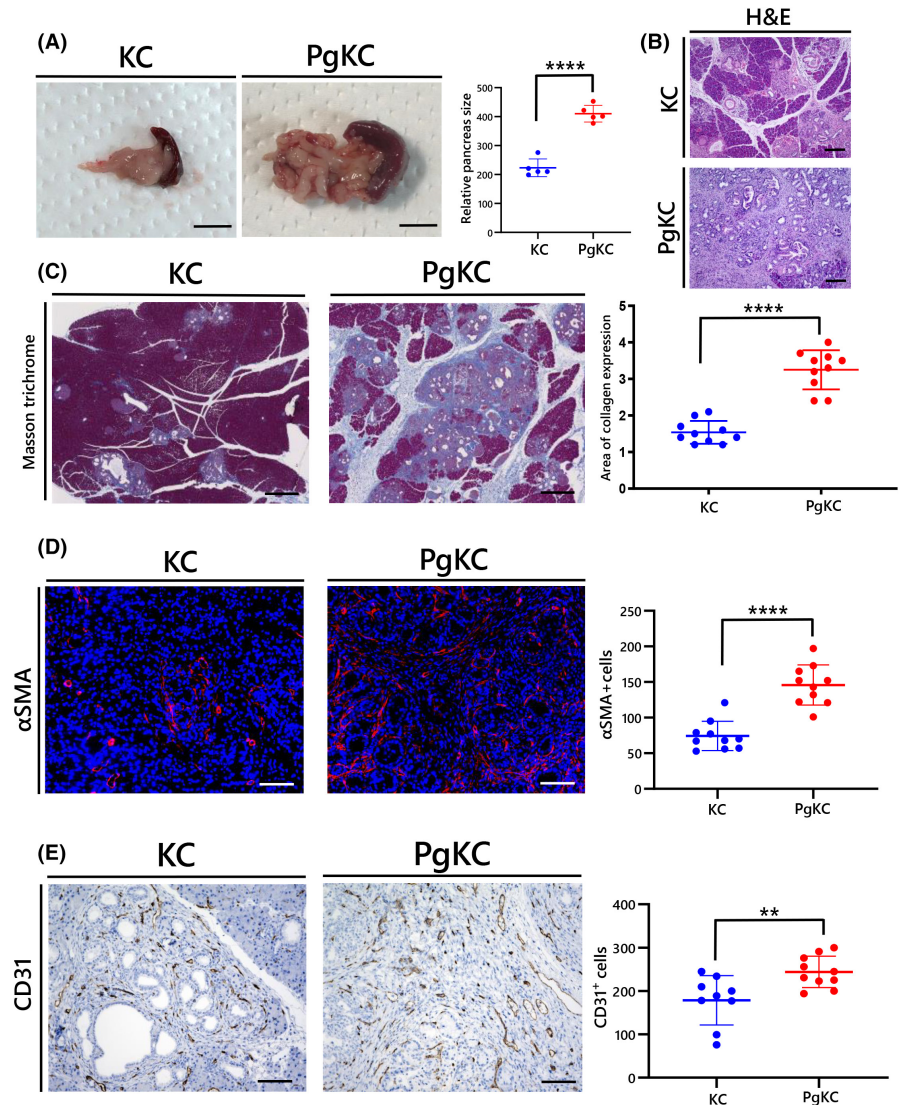
we examined the expression of FGF1 to FGF10 in cancer cells after PGE2 stimulation. Among the target genes, FGF1 showed the most significant upregulation under PGE2 treatment (Figure 3E). As the platelet-derived growth factor (PDGF) family also promotes CAF growth, we examined PDGF expression in cancer cells after PGE2 treatment and found no significant changes (Figure S2). In addition, FGF1 expression was upregulated in tumors formed from transplanted Panc02 cells in 15-pgdh$^{+/-}$ mice compared with wild-type mice (Figure 3F). To confirm the acceleration of CAF proliferation by FGF1-FGFR signaling, we cultured CAFs using PK8 CM, PGE2-treated PK8 CM and PGE2-treated PK8 CM containing the irreversible FGFR inhibitor futibatinib. Futibatinib successfully inhibited CAF proliferation in PGE2-treated PK8 CM, supporting the hypothesis that cancer-derived FGF1 boosts CAF growth (Figure 3G). This evidence clearly showed that PGE2 accumulation activates FGF1 secretion from cancer cells, consequently promoting CAF proliferation via FGF1–FGFR signaling and leading to enhanced fibrosis.

3.4 | 15-pgdh depletion in a highly fibrotic tumor microenvironment maintains the angiogenesis level

Highly fibrotic tumors tend to suppress angiogenesis; therefore, we next focused on examining tumor angiogenesis. Interestingly, nano-CT scanning of transplanted tumors from wild-type and 15-pgdh^{+/−} mice showed no significant difference in the angiogenesis level (Figure 4A), and this finding was further confirmed by CD31 staining (Figure 4B). Vascular endothelial growth factor A (VEGFA) is one of the most important proangiogenic factors secreted in human cancers[23]; therefore, we next hypothesized that increased expression of VEGFA in the tumor microenvironment favors angiogenesis maintenance. As expected, vegfa was upregulated in tumor tissue from 15-pgdh^{+/−} mice (Figure 4C). To further verify the origin of vegfa in pancreatic tumor tissue, vegfa expression in five human PDAC cell lines and 3 CAF lines was analyzed by real-time PCR. Notably, vegfa expression was much higher in CAFs than in cancer cells (Figure 4D). Moreover, to confirm the importance of vegfa originating from CAFs, we cultured human umbilical vein endothelial cells (HUVECs) in normal RPMI 1640 medium and CM from CAFs. HUVEC tube formation was robustly enhanced after culture in CAF CM (Figure 4E). HUVECs cultured in CAF CM were also treated with the humanized anti-VEGF monoclonal antibody bevacizumab, which suppressed HUVEC tube formation (Figure 4F).

The Chorioallantoic membrane (CAM) is a highly vascularized membrane found in the eggs of certain amniotes, such as birds and reptiles, and is often used to evaluate angiogenesis *in vivo*. Therefore, we next transplanted PK8 cells with or without CAFs onto CAM samples and found that vessel formation in the PK8+CAF group was much more intense than that in the PK8 cell-only group (Figure 4G). Moreover, we used an antibody against the highly specific endothelial marker VE-cadherin to label the vessels on CAM samples[24] and found that VE-cadherin was upregulated in the PK8+CAF group compared with the PK8 cell-only group, further supporting our previous data (Figure 4H). These findings suggested that angiogenesis is maintained by vegfa originating from CAFs in the tumor microenvironment.

3.5 | Whole body depletion of 15-pgdh boosts fibrosis and angiogenesis in a genetically engineered PDAC mouse model

Endogenous pancreas-specific expression of KrasG12D causes mouse pancreatic intraepithelial neoplasias (PanIN) in 12-week-old mice.[25,26] To further determine the effect of 15-pgdh ablation on the tumor microenvironment *in vivo*, we utilized our previously established 15-pgdh^{−/−}; Kras[LSL-G12D/+]; Ptf1a[Cre/+] (referred to as PgKC) mouse model that develops PDAC.[14] Comparison of Kras[LSL-G12D/+]; Ptf1a[Cre/+] mice (referred to as KC mice) with PgKC mice at 8 weeks after birth showed significant differences in tumorigenesis development and the size of the pancreas (Figure 5A). H&E staining exhibited that, in PgKC mice, mPanIN lesions with mucinous glandular structures markedly increased compared with those in KC mice (Figure 5B). Furthermore, we evaluated the pancreatic fibrosis level in KC and PgKC mice by performing Masson's trichrome staining and immunofluorescence staining of αSMA. Significant upregulation of collagen was found in PgKC mice along with drastically increased αSMA^{+} cells (Figure 5C,D). Finally, the angiogenesis level was also examined in both mice by immunohistochemical staining of CD31, and PgKC mice showed significantly elevated CD31 expression in the pancreatic microenvironment, indicating that angiogenesis was ultimately promoted by 15-pgdh depletion (Figure 5E). The enhanced angiogenesis may be strengthened in the endogenous PDAC mouse model due to the longer exposure to PGE2 accumulation than that in the transplantation mouse model. These data provided validation of our findings in the endogenous PDAC mouse model and supported our theory that depletion of 15-pgdh promotes fibrosis and angiogenesis in the tumor microenvironment.

3.6 | CAF depletion in 15-pgdh^{+/−} mice enhances cancer cell apoptosis and suppresses angiogenesis

After confirming vegfa secretion by CAFs, we next decided to examine the effects of CAF depletion using 15-pgdh^{+/−}Acta2-TK mice, which are generated by mating genetically modified B6.FVB-Tg (Acta2-TK*)1Rkl/J mice[27] with 15-pgdh^{+/−} mice. Three weeks after transplantation of Panc02 cells, tumor volumes in 15pgdh^{+/−} mice were higher than those in 15-pgdh^{+/−}Acta2-TK mice (Figure 6A,B). However, immunohistochemical staining for Ki67 did not show significant differences between the two groups (Figure 6C). Then, we assessed the apoptosis level in both genotypes of mice. Interestingly, the TUNEL assay revealed enhanced apoptosis in 15-pgdh^{+/−}Acta2-TK mice, suggesting that depletion of CAFs promoted cancer cell apoptosis (Figure 6D). Although there was almost no difference between wild-type and Acta2-TK mice due to the low amount of CAFs, depletion of CAFs was confirmed in

FIGURE 6 CAF depletion in 15-pgdh^{+/−} mice enhances cancer cell apoptosis and suppresses angiogenesis. (A, B) Panc02 cells were injected into the pancreas of 15-pgdh^{+/−} mice and 15-pgdh^{+/−}Acta2-TK mice (fibroblast-depleted mice). After 3 weeks, the mice were euthanized, and the pancreases were harvested. Images of the pancreas and spleen. Scale bars, 1 cm (A). Graph showing the main tumor area (B). (C) Representative immunohistochemical staining for Ki67 and quantification of Ki67^{+} cells in 15-pgdh^{+/−} and 15-pgdh^{+/−} Acta2-TK mouse tumors. Scale bars, 200 μm. (D) TUNEL images and quantification in 15-pgdh^{+/−} and 15-pgdh^{+/−}Acta2-TK mouse tumors. Scale bars, 50 μm. (E) Immunofluorescence staining and quantification of αSMA in 15-pgdh^{+/−} and 15-pgdh^{+/−}Acta2-TK mouse tumors. Scale bars, 200 μm. (F) The expression of col1a1 in 15-pgdh^{+/−} and 15-pgdh^{+/−}Acta2-TK mouse tumors was determined by qRT-PCR. (G) Representative immunohistochemical staining for CD31 and quantification of CD31^{+} cells in 15-pgdh^{+/−} and 15-pgdh^{+/−}Acta2-TK mouse tumors. Scale bars, 200 μm. (H) The expression of vegfa in 15-pgdh^{+/−} and 15-pgdh^{+/−}Acta2-TK mouse tumors was determined by qRT-PCR. NS, not significant; **$p < 0.01$; ***$p < 0.001$; ****$p < 0.0001$

(A)

15-pgdh+/-Acta2-TK
(**Fibroblast depletion**)

(B)

(C)

(D)

(E)

(F)

(G)

(H)
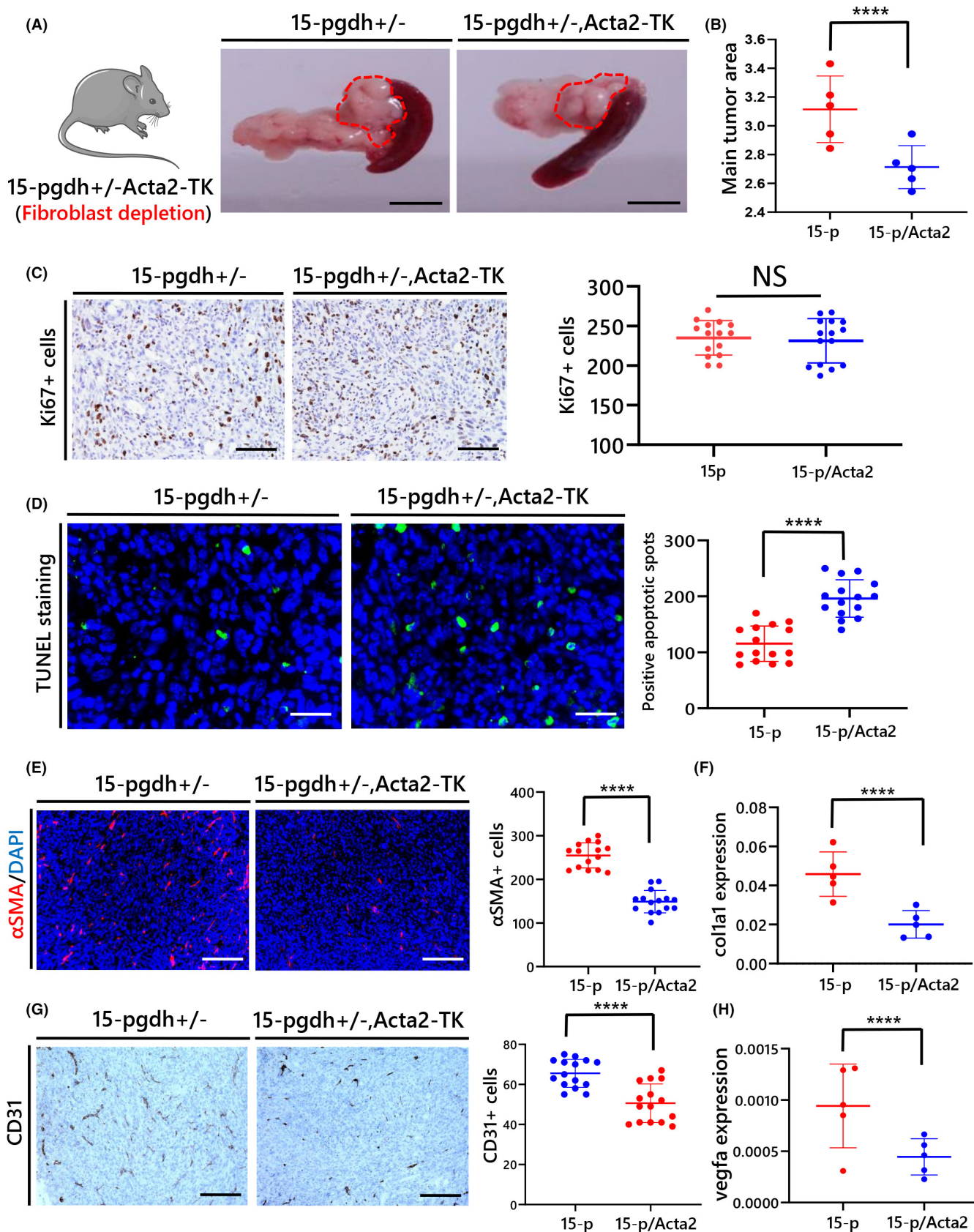
15-pgdh$^{+/-}$Acta2-TK mice by the decrease in αSMA$^+$ cells compared with those in 15pgdh$^{+/-}$ mice (Figure 6E, Figure S3), along with the downregulation of col1a1 expression at the mRNA level, indicating a reduction in fibrosis (Figure 6F). Finally, we examined angiogenesis by evaluating CD31 expression in the tumor microenvironment and the expression of vegfa. As demonstrated, CD31$^+$ cells were

decreased in 15-pgdh$^{+/-}$Acta2-TK mice (Figure 6G), accompanied by vegfa downregulation (Figure 6H). These data indicated that depletion of CAFs can suppress angiogenesis while promoting cancer cell apoptosis.

4 | DISCUSSION

Hallmarks of cancer-related inflammation include various inflammatory factors, such as cytokines, chemokines, and prostaglandins.[28,29] Moreover, well known inflammation-related pathways, such as the NF-κB, STAT3 and MAPK pathways, are also activated during cancer progression.[30,31] To date, our understanding of cancer-related inflammation has led to the development of numerous approaches for cancer prevention and anticancer treatment.[32] Among the anticancer agents targeting inflammation-related genes, COX-2 inhibitors have continued to emerge in recent decades and have been reported to reduce cancer-associated mortality.[33] As a very common eicosanoid, PGE2 is largely considered to be one of the most essential factors that can regulate stem cell homeostasis; for example, it has been found to accelerate hematopoietic stem cell proliferation in both mice and zebrafish.[11,12] In addition, PGE2 is the most abundant prostaglandin that has been found in various human malignancies and plays a crucial role in various cancers. Similar to its effects on tissue stem cells, PGE2 accumulation has a massive impact on increasing the cancer stem cell population; as we previously reported, it can boost cancer cell proliferation via activation of ALDH1, and this finding is similar to that of another study that demonstrated that PGE2 induces cancer stem cell expansion via PI3K/MAPK signaling.[14,34] Moreover, immunosuppression mediated by PGE2 is another main topic of notable focus in the past few years. In nonmalignant but highly inflammatory diseases such as liver cirrhosis, innate immune impairment is mediated by PGE2,[35] whereas in malignant diseases, antitumor immunity is suppressed by PGE2, for example, through senescent hepatic stellate cells in liver cancer.[36] In addition, by selectively binding to EP2/EP4 receptors on natural killer (NK) cells, PGE2 can enable immune evasion, therefore promoting cancer progression.[37] In a recent study, PGE2 was reported to activate an Akt-fibroblast growth factors (FGF)-2/TGF-β/VEGF proangiogenic pathway in glioma.[38] Despite the several notable roles of PGE2 in cancer cells, the precise consequences of its accumulation in the tumor microenvironment are incompletely known. In the current study, we demonstrated that PGE2 accumulation caused by 15-PGDH inhibition can lead to activation of FGF1 secretion from cancer cells, subsequently leading to enhancement of CAF proliferation and tissue fibrosis.

Although several studies have reported 15-PGDH to be a tumor suppressor in various cancers by promoting antitumor immunity or suppressing cancer cell proliferation,[15,16] few studies have shown the origin of 15-pgdh in the tumor microenvironment. We have previously shown that 15-PGDH can be expressed by PDAC cells and downregulated by IL-1β derived from activated macrophages, indicating that 15-PGDH can be expressed by PDAC cells[22]; however, its predominant source remained unclear. Recent studies have shown that 15-pgdh is highly expressed by Tregs and macrophages in visceral adipose tissue and muscle microenvironments.[20,21] In addition to these findings in normal tissues, we demonstrated that 15-PGDH is expressed predominantly by macrophages in the tumor microenvironment and that depletion of 15-pgdh remodeled the microenvironment and subsequently enhanced pancreatic tumor development.

PDAC not only is considered to have a highly fibrotic tumor microenvironment but also usually exhibits hypovascularity and vascular compression.[39] In a PDAC model mice, such as mice harboring endogenous mutant Kras and p53 alleles in pancreatic cells (KPC mice), pancreatic tumors are characterized by hypovascularity and robust pancreatic desmoplasia.[40] Conversely, angiogenesis is the process by which new capillaries grow from preexisting blood vessels and is essential for the growth and metastasis of many solid tumors, including pancreatic cancer.[41] Although PDAC tumors are often hypovascular, recent studies have indicated that in a fibrotic tumor microenvironment, enhanced angiogenesis can be found in liver metastasis sites of colon cancer and that targeting the renin–angiotensin system can reduce tissue stiffness and increase antiangiogenic drug efficacy.[42] Among the already identified proangiogenic molecules, VEGFA is considered a key regulatory mediator of pathological blood vessel growth and maintenance.[43] Here, we provide evidence showing that in the highly fibrotic PDAC tumor microenvironment, PGE2 stimulates cancer cells to secrete FGF1, which promotes CAF proliferation, subsequently increases the level of CAF-derived VEGFA and maintains the angiogenesis level. In our syngeneic transplantation model, the angiogenesis level was maintained in the highly fibrotic tumor microenvironment after 15-pgdh depletion; however, in the endogenous 15-pgdh knockout KC mouse, the angiogenesis level was enhanced. This phenomenon can be explained by the time gap in development between the two types of models: in the transplantation model, the vessels only developed for 3 weeks, whereas in the endogenous mouse model, they developed for 8 weeks. In addition, the possibility that the amount of accumulated PGE2 in 15-pgdh$^{-/-}$ mice can exceed that in 15-pgdh$^{+/-}$ mice should also be taken into consideration. Finally, depletion of CAFs in 15-pgdh$^{+/-}$Acta2-TK mice reversed this phenomenon, as both angiogenesis and fibrosis decreased.

In summary, our study presents a novel role of 15-PGDH in the tumor microenvironment. 15-PGDH is expressed predominantly by macrophages in the PDAC tumor microenvironment, and depletion of 15-PGDH leads to PGE2 accumulation. PGE2 accumulation subsequently activates FGF1 secretion by cancer cells, which promotes CAF proliferation and fibrosis, eventually resulting in VEGFA elevation and angiogenesis enhancement. These findings add important insights into our understanding of the pancreatic cancer tumor microenvironment and will ultimately contribute to the development of alternative therapeutic strategies for PDAC.

DISCLOSURE

The authors declare no potential conflicts of interest.

ETHICAL APPROVAL

This study was approved by the Ethical Review Board of the Graduate School of Medicine, Kumamoto University (Approval no. 1291), and informed consent for the use of medical records was obtained from each patient. All animal experimental protocols were approved by the Ethical Review Board of the Graduate School of Medicine, Kumamoto University (Approval no. 2020-018R1).

PERMISSION TO REUSE AND COPYRIGHT

The figures were partially created using BioRender.com.

ORCID

Toshiro Moroishi https://orcid.org/0000-0001-6419-3882
Hideo Baba https://orcid.org/0000-0002-3474-2550
Takatsugu Ishimoto https://orcid.org/0000-0003-1852-1835

REFERENCES

1. Mizrahi JD, Surana R, Valle JW, Shroff RT. Pancreatic cancer. *Lancet*. 2020;395(10242):2008-2020.
2. Bray F, Ferlay J, Soerjomataram I, Siegel RL, Torre LA, Jemal A. Global cancer statistics 2018: GLOBOCAN estimates of incidence and mortality worldwide for 36 cancers in 185 countries. *CA Cancer J Clin*. 2018;68(6):394-424.
3. Kamisawa T, Wood LD, Itoi T, Takaori K. Pancreatic cancer. *Lancet*. 2016;388(10039):73-85.
4. Gillen S, Schuster T, Meyer Zum Buschenfelde C, Friess H, Kleeff J. Preoperative/neoadjuvant therapy in pancreatic cancer: a systematic review and meta-analysis of response and resection percentages. *PLoS Med*. 2010;7(4):e1000267.
5. Ritter B, Greten FR. Modulating inflammation for cancer therapy. *J Exp Med*. 2019;216(6):1234-1243.
6. Whatcott CJ, Diep CH, Jiang P, et al. Desmoplasia in primary tumors and metastatic lesions of pancreatic cancer. *Clin Cancer Res*. 2015;21(15):3561-3568.
7. Yadav D, Lowenfels AB. The epidemiology of pancreatitis and pancreatic cancer. *Gastroenterology*. 2013;144(6):1252-1261.
8. Alexandre M, Pandol SJ, Gorelick FS, Thrower EC. The emerging role of smoking in the development of pancreatitis. *Pancreatology*. 2011;11(5):469-474.
9. Sempere L, Martinez J, de Madaria E, et al. Obesity and fat distribution imply a greater systemic inflammatory response and a worse prognosis in acute pancreatitis. *Pancreatology*. 2008;8(3):257-264.
10. Wang D, Dubois RN. Eicosanoids and cancer. *Nat Rev Cancer*. 2010;10(3):181-193.
11. Zhang Y, Desai A, Yang SY, et al. TISSUE REGENERATION. Inhibition of the prostaglandin-degrading enzyme 15-PGDH potentiates tissue regeneration. *Science*. 2015;348(6240):aaa2340.
12. North TE, Goessling W, Walkley CR, et al. Prostaglandin E2 regulates vertebrate haematopoietic stem cell homeostasis. *Nature*. 2007;447(7147):1007-1011.
13. Wang D, DuBois RN. Role of prostanoids in gastrointestinal cancer. *J Clin Invest*. 2018;128(7):2732-2742.
14. Arima K, Ohmuraya M, Miyake K, et al. Inhibition of 15-PGDH causes Kras-driven tumor expansion through prostaglandin E2-ALDH1 signaling in the pancreas. *Oncogene*. 2019;38(8):1211-1224.
15. Prima V, Kaliberova LN, Kaliberov S, Curiel DT, Kusmartsev S. COX2/mPGES1/PGE2 pathway regulates PD-L1 expression in tumor-associated macrophages and myeloid-derived suppressor cells. *Proc Natl Acad Sci USA*. 2017;114(5):1117-1122.
16. Kim HB, Kim M, Park YS, et al. Prostaglandin E2 activates YAP and a positive-signaling loop to promote colon regeneration after colitis but also carcinogenesis in mice. *Gastroenterology*. 2017;152(3):616-630.
17. Yamao T, Yamashita YI, Yamamura K, et al. Cellular senescence, represented by expression of Caveolin-1, in cancer-associated fibroblasts promotes tumor invasion in pancreatic cancer. *Ann Surg Oncol*. 2019;26(5):1552-1559.
18. Yasuda T, Koiwa M, Yonemura A, Akiyama T, Baba H, Ishimoto T. Protocol to establish cancer-associated fibroblasts from surgically resected tissues and generate senescent fibroblasts. *STAR Protoc*. 2021;2(2):100553.
19. Coggins KG, Latour A, Nguyen MS, Audoly L, Coffman TM, Koller BH. Metabolism of PGE2 by prostaglandin dehydrogenase is essential for remodeling the ductus arteriosus. *Nat Med*. 2002;8(2):91-92.
20. Schmidleithner L, Thabet Y, Schonfeld E, et al. Enzymatic activity of HPGD in Treg cells suppresses Tconv cells to maintain adipose tissue homeostasis and prevent metabolic dysfunction. *Immunity*. 2019;50(5):1232-48 e14.
21. Palla AR, Ravichandran M, Wang YX, et al. Inhibition of prostaglandin-degrading enzyme 15-PGDH rejuvenates aged muscle mass and strength. *Science*. 2021;371(6528):eabc8059.
22. Arima K, Komohara Y, Bu L, et al. Downregulation of 15-hydroxyprostaglandin dehydrogenase by interleukin-1beta from activated macrophages leads to poor prognosis in pancreatic cancer. *Cancer Sci*. 2018;109(2):462-470.
23. Senger DR, Van de Water L, Brown LF, et al. Vascular permeability factor (VPF, VEGF) in tumor biology. *Cancer Metastasis Rev*. 1993;12(3–4):303-324.
24. Arraf AA, De Bruijn M, Schultheiss TM. Disruption of the aortic wall by coelomic lining-derived mesenchymal cells accompanies the onset of aortic hematopoiesis. *Int J Dev Biol*. 2017;61(3–4-5):329-335.
25. Hingorani SR, Petricoin EF, Maitra A, et al. Preinvasive and invasive ductal pancreatic cancer and its early detection in the mouse. *Cancer Cell*. 2003;4(6):437-450.
26. Hruban RH, Adsay NV, Albores-Saavedra J, et al. Pathology of genetically engineered mouse models of pancreatic exocrine cancer: consensus report and recommendations. *Cancer Res*. 2006;66(1):95-106.
27. LeBleu VS, Taduri G, O'Connell J, et al. Origin and function of myofibroblasts in kidney fibrosis. *Nat Med*. 2013;19(8):1047-1053.
28. Diakos CI, Charles KA, McMillan DC, Clarke SJ. Cancer-related inflammation and treatment effectiveness. *Lancet Oncol*. 2014;15(11):e493-e503.
29. Mantovani A, Allavena P, Sica A, Balkwill F. Cancer-related inflammation. *Nature*. 2008;454(7203):436-444.
30. Taniguchi K, Karin M. NF-kappaB, inflammation, immunity and cancer: coming of age. *Nat Rev Immunol*. 2018;18(5):309-324.
31. Koliaraki V, Pasparakis M, Kollias G. IKKbeta in intestinal mesenchymal cells promotes initiation of colitis-associated cancer. *J Exp Med*. 2015;212(13):2235-2251.
32. Crusz SM, Balkwill FR. Inflammation and cancer: advances and new agents. *Nat Rev Clin Oncol*. 2015;12(10):584-596.
33. Cuzick J. Preventive therapy for cancer. *Lancet Oncol*. 2017;18(8):e472-e482.
34. Wang D, Fu L, Sun H, Guo L, DuBois RN. Prostaglandin E2 promotes colorectal cancer stem cell expansion and metastasis in mice. *Gastroenterology*. 2015;149(7):1884-95 e4.

35. O'Brien AJ, Fullerton JN, Massey KA, et al. Immunosuppression in acutely decompensated cirrhosis is mediated by prostaglandin E2. *Nat Med*. 2014;20(5):518-523.

36. Loo TM, Kamachi F, Watanabe Y, et al. Gut microbiota promotes obesity-associated liver cancer through PGE2-mediated suppression of antitumor immunity. *Cancer Discov*. 2017;7(5):522-538.

37. Bonavita E, Bromley CP, Jonsson G, et al. Antagonistic inflammatory phenotypes dictate tumor fate and response to immune checkpoint blockade. *Immunity*. 2020;53(6):1215-29 e8.

38. Wang C, Chen Y, Wang Y, et al. Inhibition of COX-2, mPGES-1 and CYP4A by isoliquiritigenin blocks the angiogenic Akt signaling in glioma through ceRNA effect of miR-194-5p and lncRNA NEAT1. *J Exp Clin Cancer Res*. 2019;38(1):371.

39. Hessmann E, Buchholz SM, Demir IE, et al. Microenvironmental determinants of pancreatic cancer. *Physiol Rev*. 2020;100(4):1707-1751.

40. Olive KP, Jacobetz MA, Davidson CJ, et al. Inhibition of hedgehog signaling enhances delivery of chemotherapy in a mouse model of pancreatic cancer. *Science*. 2009;324(5933):1457-1461.

41. Folkman J. What is the evidence that tumors are angiogenesis dependent? *J Natl Cancer Inst*. 1990;82(1):4-6.

42. Shen Y, Wang X, Lu J, et al. Reduction of liver metastasis stiffness improves response to bevacizumab in metastatic colorectal cancer. *Cancer Cell*. 2020;37(6):800-17 e7.

43. Ellis LM, Hicklin DJ. VEGF-targeted therapy: mechanisms of antitumour activity. *Nat Rev Cancer*. 2008;8(8):579-591.

SUPPORTING INFORMATION

Additional supporting information can be found online in the Supporting Information section at the end of this article.